ELSEVIER

Flow Measurement and Instrumentation 12 (2001) 135–145

Flow Measurement and Instrumentation

www.elsevier.com/locate/flowmeasinst

Discharge coefficients of Venturi tubes with standard and non-standard convergent angles

M.J. Reader-Harris *, W.C. Brunton, J.J. Gibson, D. Hodges, I.G. Nicholson

National Engineering Laboratory, East Kilbride, Scotland G75 0QU, UK

Abstract

This paper describes twenty one Venturi tubes manufactured in a range of diameter ratios from 0.4 to 0.75. Fifteen of them are standard, with a convergent angle of 21°, manufactured in a range of diameters from 50 mm to 200 mm and of diameter ratios from 0.4 to 0.75. Six are standard except for the convergent angles which are either 10.5° or 31.5°; they are of diameter 100 mm. They have all been calibrated in water and high-pressure gas. For the standard Venturi tubes an equation for the discharge coefficient in water has been obtained with an uncertainty of 0.74 per cent. Work on the physical basis of the equation for the discharge coefficient at high Reynolds number is described, and an equation fitting all the gas data from the standard Venturi tubes with an uncertainty of 1.23 per cent has been derived. It is clear that the data in gas from the Venturi tubes with a convergent angle of 10.5° are much smoother than those from Venturi tubes with the standard or the higher convergent angle: an equation fitting all the gas data from the three Venturi tubes with a convergent angle of 10.5° has been obtained with an uncertainty of 0.71 per cent.

Keywords: Flow measurement; Differential pressure meters; Venturi tubes

1. Introduction

There is an increasing desire to use Venturi tubes for wet gas measurement, but to ensure accuracy it is necessary to understand their behaviour in dry gas first. However, the work of Jamieson et al. [1] and of van Weers et al. [2] has shown that their performance in gas is very different from that in water. This project is being undertaken to examine the performance of a range of Venturi tubes whose manufacture was carefully specified and controlled. One way of improving the results in high-pressure gas is to change the design of the Venturi tube. The option of changing the convergent angle is described here. This work is a fuller version of part of that described in References [3] and [4].

2. Description of the Venturi tubes

Fifteen classical Venturi tubes with machined convergent sections were manufactured by Jordan Kent Metering Systems/Seiko and Crane Perflow for calibration in water and in gas: the former manufacturer manufactured Venturi tubes with diameter ratio β=0.4, 0.6 and 0.75 for nominal diameter 50 mm, 100 mm and 200 mm, together with β=0.5, 0.65 and 0.7 for nominal diameter 100 mm only; the latter manufactured Venturi tubes with β=0.4, 0.6 and 0.75 for nominal diameter 100 mm only. Six additional Venturi tubes with machined convergent sections were manufactured by Jordan Kent Metering Systems/Seiko for calibration in water and in gas with diameter ratio β=0.4, 0.6 and 0.75 and nominal diameter 100 mm. They were standard Venturi tubes except that three had a convergent angle of 10.5° and three had a convergent angle of 31.5°. They were manufactured to drawings with tight tolerances designed to ensure that where possible the results were not affected by uncontrolled variables. Each Venturi tube was manufactured out of solid metal so that there would be no steps due to welding within the Venturi tube. They were made of stainless steel and were suitable for use at pressures up to 70 bar with ANSI Class 600 flanges. They were designed not only to meet the requirements of ISO 5167-1 [5] but to follow its recommendations. The Standard recommends the use of a divergent angle between 7° and 8°: $7\frac{1}{2}$° was specified for the Venturi tubes used in this project.

* Corresponding author. Tel.: +44-1355-272302; fax: +44-1355-272536.

E-mail address: mreader@nel.uk (M.J. Reader-Harris).

0955-5986/01/$ - see front matter
PII: S0955-5986(01)00007-3

Nomenclature

C	Discharge coefficient
C_{water}	Mean discharge coefficient in water
D	Diameter of entrance cylinder, m
d	Throat diameter, m
d_{tap}	Tapping hole diameter, m
e	Change in measured pressure, Pa
k	Uniform equivalent roughness (as on the Moody diagram), m
R_a	Arithmetic mean deviation of the roughness profile, m
Re_D	Pipe Reynolds number
Re_d	Throat Reynolds number
Re_{tap}	Tapping hole Reynolds number ($=u_\tau d_{tap}/\nu$)
Re^*	Venturi throat tapping Reynolds number ($=Re_d d_{tap}/d$)
$\bar{u}$	Mean velocity, m/s
u_τ	Friction velocity ($=\sqrt{(\tau/\rho)}$), m/s
β	Diameter ratio ($=d/D$)
λ	Friction factor
ν	Kinematic viscosity, m^2/s
ρ	Density, kg/m^3
τ	Wall shear stress, Pa

So that the results would not be corrupted by the introduction of steps at joins in the pipework, an upstream length of 8D (6D for 200 mm pipe) and a downstream length of 4D, where D is the diameter of the entrance cylinder, were manufactured with machined bores; this ensured that in no case was there a step in diameter greater than 0.0035D at the upstream flange of the Venturi tube. The lengths of pipework were manufactured by boring out Schedule 80 pipe to the bore of a Schedule 40 pipe. The lengths of pipe and the Venturi tubes were dowelled to ensure concentricity; O rings were used to ensure that there would not be recesses or protruding gaskets. The distance from the upstream pressure tappings to the first upstream flange was 1.5D, 1.1D and 0.7D for nominal diameters of 50 mm, 100 mm and 200 mm respectively.

In addition to the shorter lengths of pipework already described, an additional 21D (23D of 200 mm pipe) length was manufactured by welding a 19D (21D of 200 mm pipe) length of Schedule 40 pipe to a 2D length of pipe machined to the bore of the other pipes, smoothing off any step at the weld. This length of pipe was installed with the machined length adjacent to the machined pipe already described, so that there was at least 8D of machined pipework, whose bore matched that of the Venturi tube very accurately, immediately upstream of the Venturi tube. In total there was 29D of pipe of the same schedule with no recesses, protruding gaskets or significant steps upstream of the Venturi tube. Upstream of this assembly there was generally further pipe of the same nominal diameter preceded by a flow conditioner.

The Standard recommends that the radii of curvature at the intersections of the entrance cylinder and the convergent section, the convergent section and the throat, and the throat and the divergent section be equal to zero, although significantly larger values are permitted. The drawings requested a maximum radius of curvature of 1 mm. In order to measure the radius of curvature, measurements of profile were made through the convergent and the throat with one trace per Venturi tube. This was not possible for some of the Venturi tubes. The average of the measured radii of curvature was 15 mm. Some radii of curvature were outside the permitted value of 0.25d, but the range of radii of curvature does not appear to be the cause of the spread in measured discharge coefficients.

The Standard requires that the surface finish of the entrance cylinder, the convergent section and the throat be such that R_a/d shall always be less than 10^{-5}, where R_a is the arithmetical mean deviation of the roughness profile. However, this was typically exceeded by a factor of approximately 3; the typical surface finish was $R_a \approx 2$ μm. All the Venturi tubes had $10^{-5} < R_a/d < 10^{-4}$. If the Draft International Standard proposed to replace ISO 5167-1 is accepted the maximum permissible roughness will be increased so that R_a/d shall be less than 10^{-4}. The project wished to use Venturi tubes with surface roughnesses typical of those used in the field. Moreover, the range of roughnesses does not appear to be the cause of the spread in measured discharge coefficients.

Except for the Venturi tube with a throat diameter of 20 mm the pressure tappings were 4 mm in diameter; the throat pressure tappings were of constant diameter for a length of 94 mm and the upstream tappings for a

length of 53 mm. The Venturi tube with a throat diameter of 20 mm had pressure tappings of diameter 2.6 mm; the throat pressure tappings were of constant diameter for a length of 62 mm and the upstream tappings for a length of 37 mm. Tappings of constant diameter were used because the work described by Jamieson et al. [1] suggested that they might be beneficial. The tappings were connected in "triple-tee" arrangements.

For most of the Venturi tubes the convergent angles were determined both from three measurements of diameter for each convergent cone and from the wall profile measurements from which the intersection radii were obtained. The measured value of the convergent angle never differed from the nominal value by more than 0.14°.

Except for one measured diameter in the 20 mm throat (nominal diameter 50 mm, β=0.4), the measured throat diameters were within 0.1 per cent of the mean value of the throat diameters at the pressure tappings. The measured diameters of the entrance cylinders were within 0.075 per cent of the mean value of the entrance cylinder diameters at the pressure tappings.

3. Calibration in water

The Venturi tubes were calibrated in water in the UKAS-accredited National Standard facility for water flow measurement. For each Venturi tube the data in water lay on a straight line and with a small scatter. The gradients were small: when fitted against Re_D the majority had a positive gradient but since several had a negative gradient it seemed appropriate to represent the discharge coefficient of each Venturi tube by its mean value. Over the range of the data the average increase in discharge coefficient with Reynolds number was 0.0007. The results for the standard Venturi tubes are shown in Fig. 1. Where two Venturi tubes are made from the same drawings the maximum difference in mean discharge coefficient is 0.57 per cent. The Reynolds number range over which the data were used to calculate the mean was that over which C was approximately constant. In one case there was a significant hump in the data for $1.2\times10^5<Re_D<2\times10^5$; the throat Reynolds number below which C decreased rapidly varied but was typically about 2.5×10^5.

Fitting the data in Fig. 1 gives an equation for C in water of

$$C_{water}=0.9878+0.0123\beta. \quad (1)$$

This equation has an uncertainty (based on two standard deviations) of 0.74 per cent.

The data from the non-standard Venturi tubes are shown in Fig. 2. For comparison Eq. (1) is shown. The discharge coefficients of the Venturi tubes with a convergent angle of 10.5° are smaller than those with the standard angle owing to the additional pressure loss in the longer throat. The discharge coefficients of the Venturi tubes with a convergent angle of 31.5° are also smaller than those with the standard angle. This may be due to separation at the downstream end of the convergent section.

The non-standard Venturi tubes together with five with standard convergent angles were calibrated in water both in the NEL Water Bay and in the NEL Multiphase Flow Facility. The two Venturi tubes with convergent angle 31.5° and diameter ratios 0.6 and 0.75 gave results significantly different from the pattern of results taken with the other nine Venturi tubes. They have discharge coefficients which are higher in the Multiphase Flow Facility than in the Water Bay. Perhaps for some reason the flow separated in the throat of the Venturi tube in the Water Bay but not in the Multiphase Flow Facility. Perhaps Venturi tubes with convergent angles significantly larger than the standard value give less repeatable results than ones with the standard convergent angle.

4. Calibration in gas

The Venturi tubes were calibrated in gas in the UKAS-accredited National Standard facility for high-pressure gas flow measurement at two static pressures, 20 bar and 60 (or 70) bar, and the data from those with the standard convergent angle are presented in Figs. 3–

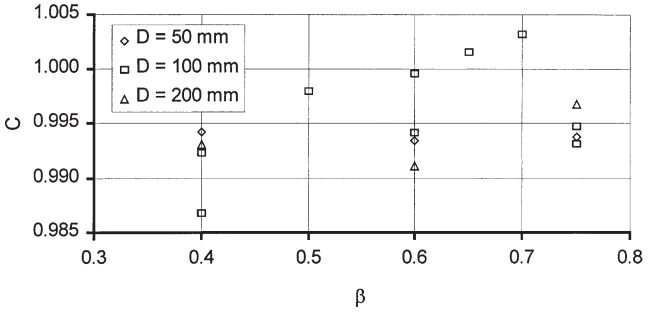

Fig. 1. Mean discharge coefficients in water: standard convergent angle.

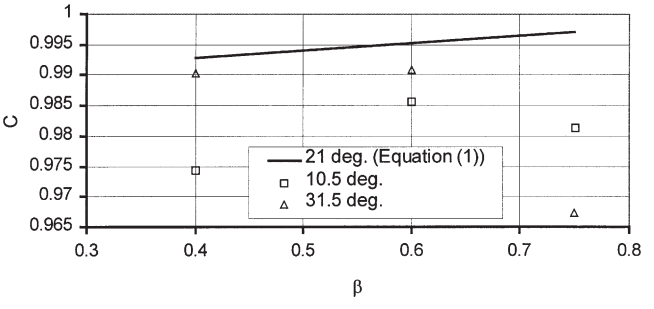

Fig. 2. Mean discharge coefficients in water: non-standard convergent angles.

6. All the gas data were collected in air except the data for 100 mm for β=0.4 from Jordan Kent Metering Systems/Seiko, which were collected in nitrogen. Since there are two 100 mm Venturi tubes for β=0.4, 0.6 and 0.75, the ones from Jordan Kent Metering Systems/Seiko are described as "100 mm" and those from Crane Perflow are described as "100 mm*". In Fig. 5(a) and (b) "Yokogawa DP" and "Mensor DP" refer to the devices used to measure the differential pressure; they were used for two separate calibrations. The data collected in gas are more scattered than those taken in water. There are peaks and troughs in the data sets. In general better agreement is obtained between the two sets of data obtained at different static pressures when the data are fitted against Reynolds number; however, it is clear that the location of the peaks and troughs is a function of the throat velocity. This can be seen in Figs. 3–6, or more clearly, since there are fewer points, in Figs. 7–9. The points for which $\Delta p/p_1 > 0.08$ were omitted from the curve fitting in this paper since these points displayed a reduction in discharge coefficient from what would have been expected from other data from the same Venturi

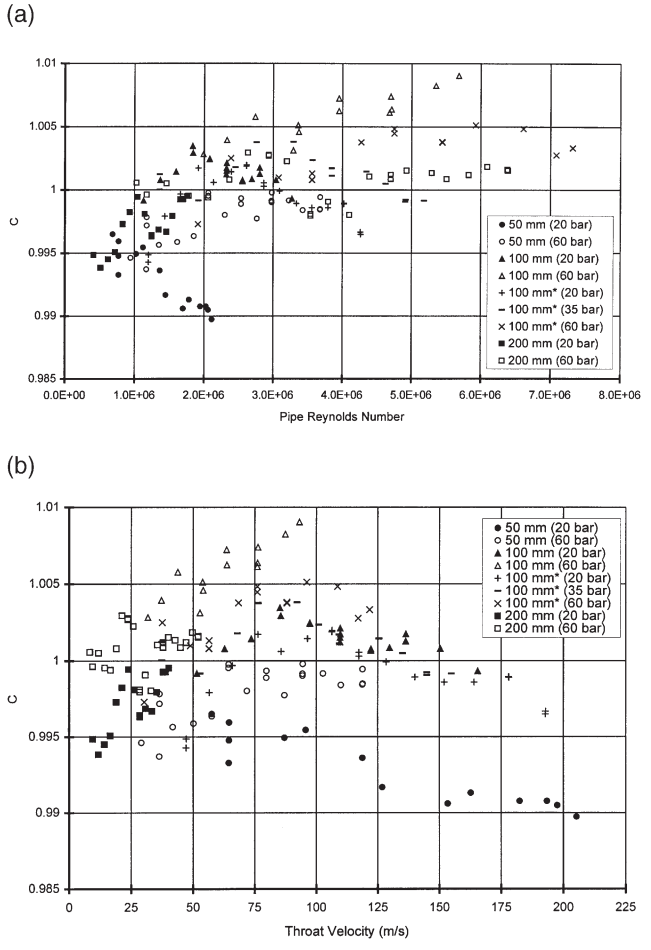

Fig. 3. (a) Calibration in gas against Reynolds number: β=0.4, standard convergent angle; (b) Calibration in gas against throat velocity: β=0.4, standard convergent angle.

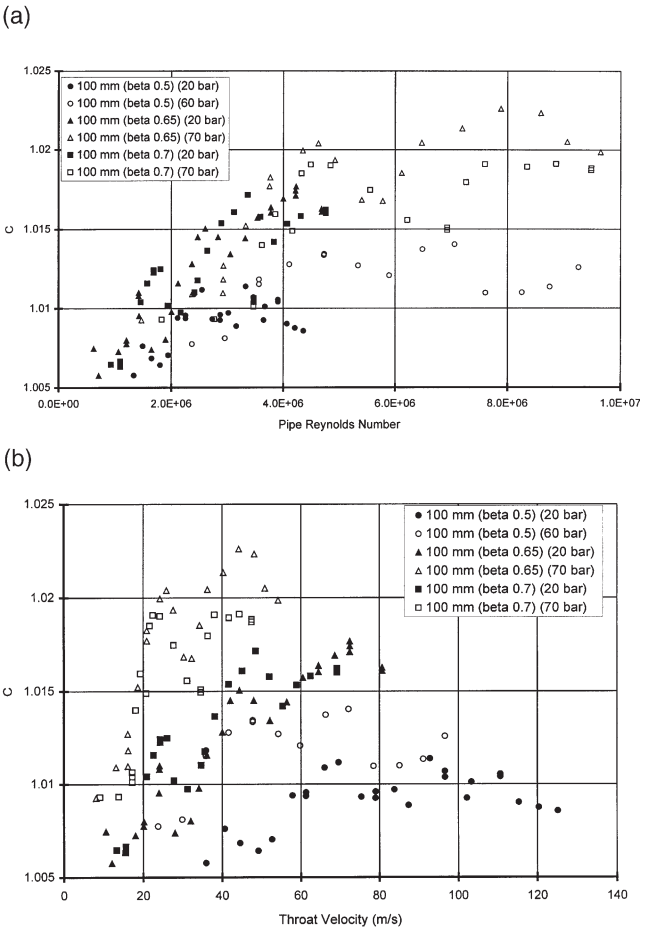

Fig. 4. (a) Calibration in gas against Reynolds number: β=0.5, 0.65 and 0.7, standard convergent angle; (b) Calibration in gas against throat velocity: β=0. 5, 0.65 and 0.7, standard convergent angle.

tube. It is assumed that this effect is due to expansibility effects which are not incorporated in the expansibility equation. The difference is, however, less than the predicted uncertainty of ε_1 in ISO 5167-1.

The data for non-standard convergent angles are presented in Figs. 7–9. The peaks and troughs are larger in the data for a convergent angle of 31.5° than in those for one of 10.5°. In the former case there are throat velocities near which the discharge coefficient changes rapidly.

5. Static hole error

In order to fit the gas data it is helpful to observe that some of the variation in C can be removed by examining $C - C_{\text{water}}$ where C_{water} is the mean value for the water data for that Venturi tube as shown in Fig. 1 or 2. A possible cause for the change in discharge coefficient from that obtained in water is static hole error. Static hole error is the effect that pressure tappings of finite size do not measure the pressure which would have been

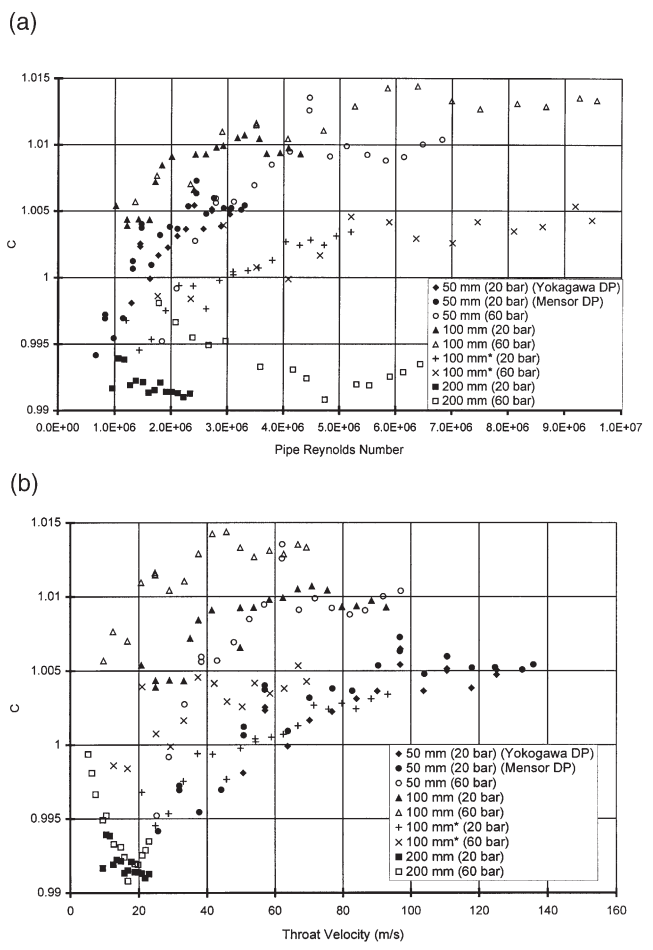

Fig. 5. (a) Calibration in gas against Reynolds number: β=0.6, standard convergent angle; (b) Calibration in gas against throat velocity: β=0.6, standard convergent angle.

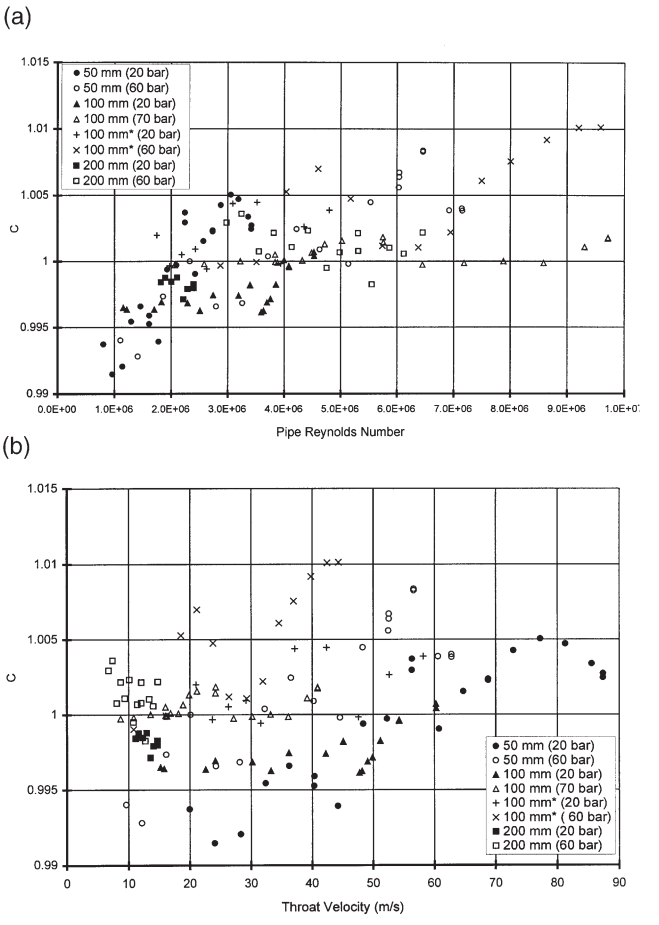

Fig. 6. (a) Calibration in gas against Reynolds number: β=0.75, standard convergent angle; (b) Calibration in gas against throat velocity: β=0.75, standard convergent angle.

measured using an infinitely small hole. The effect of static hole error is that the measured pressure using a pressure tapping is higher than the static pressure would have been if the tapping had not been present. This effect is considered in many papers (e.g. Franklin and Wallace [6] and Gibson et al. [7]). If the increase in measured pressure is denoted by e and the wall shear stress by τ, then

$$\frac{e}{\tau}=f(Re_{\text{tap}}), \tag{2}$$

where Re_{tap} is the tapping hole Reynolds number defined by

$$Re_{\text{tap}}=\frac{u_\tau d_{\text{tap}}}{\nu}, \tag{3}$$

d_{tap} is the tapping diameter, ν is the kinematic viscosity, u_τ is the friction velocity, $\sqrt{(\tau/\rho)}$, and ρ is the density. Because the velocity and therefore the wall shear stress are much higher in the throat than in the entrance cylinder, the static hole error leads to a reduction in the measured differential pressure and an increase in the measured value of C. To calculate the static hole error it is necessary to have an estimate of the relationship between τ and $\bar{u}$, the mean velocity at the tapping plane. Following Schlichting [8], this is expressed in terms of the friction factor, λ, where

$$\tau=\tfrac{1}{8}\lambda\rho\bar{u}^2. \tag{4}$$

In a standard Venturi tube, in both tapping planes Lindley [9] made measurements of τ from which λ can be deduced. Lindley showed that in the entrance cylinder λ appears to be becoming asymptotic to 0.012 as Reynolds number increases. For $10^6<Re_{\text{D}}<10^7$ and $k/D=5\times10^{-5}$, λ will always be within 10 per cent of 0.012 in a straight pipe according to the Moody Diagram (see Schlichting); so it seems an appropriate value to use. In the throat, Lindley's measurements of λ are approximately 18 per cent higher than would be obtained in a straight pipe of the same relative roughness and Reynolds number; so in determining the static hole error a figure of 0.015 has been used (for $10^6<Re_{\text{d}}$ and

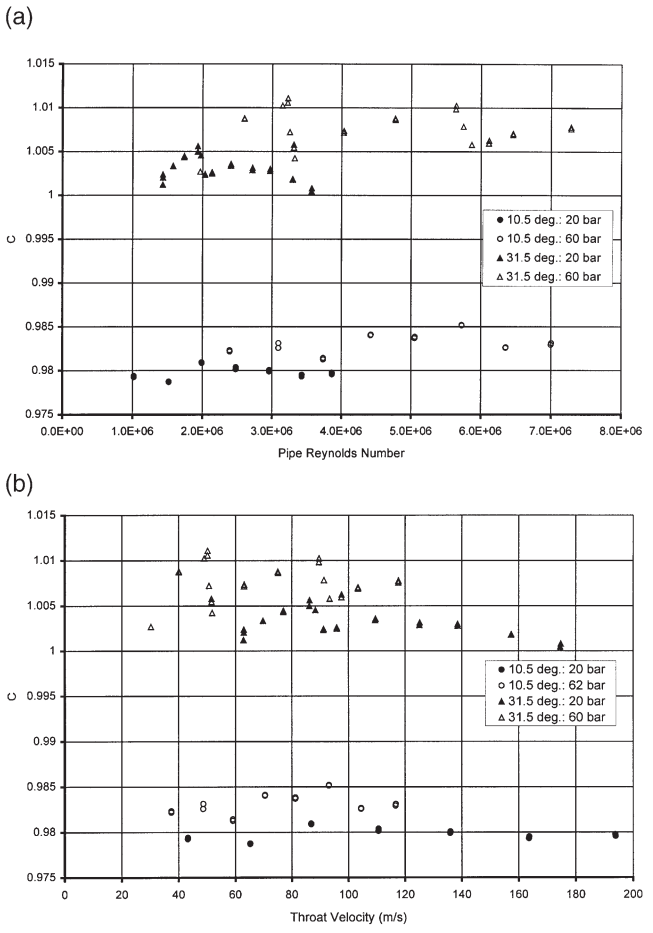

Fig. 7. (a) Calibration in gas against Reynolds number: β=0.4, 100 mm, non-standard convergent angles; (b) Calibration in gas against throat velocity: β=0.4, 100 mm, non-standard convergent angles.

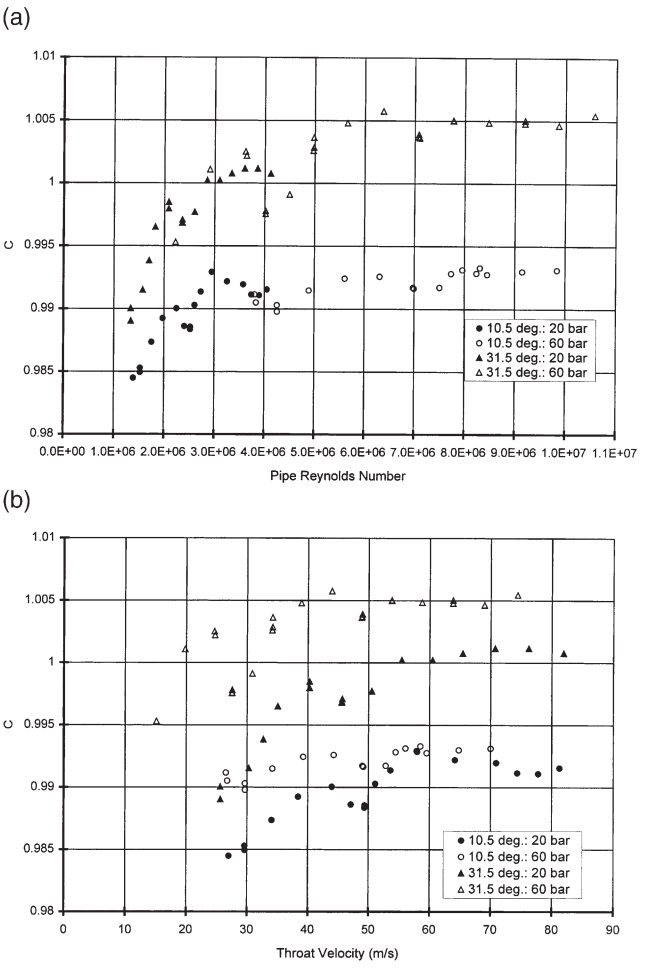

Fig. 8. (a) Calibration in gas against Reynolds number: β=0.6, 100 mm, non-standard convergent angles; (b) Calibration in gas against throat velocity: β=0.6, 100 mm, non-standard convergent angles.

$k/d=10^{-4}$, 1.18λ will always be within 6 per cent of 0.015 according to the Moody Diagram).

On this basis (and assuming incompressible flow) the predicted value of the total reduction in differential pressure, e_{total}, is given by

$$e_{\text{total}}=\tfrac{1}{8}\bar{u}^2_{\text{throat}}\rho(0.015f(Re_{\text{tap,throat}})-0.012\beta^4 f(Re_{\text{tap,up}})), \quad (5)$$

This corresponds to an increase in discharge coefficient of approximately

$$\frac{0.015f(Re_{\text{tap,throat}})-0.012\beta^4 f(Re_{\text{tap,up}})}{8(1-\beta^4)} \quad (6)$$

In deriving an equation it is necessary to consider the change in C from that found in water. Towards the higher end of the Reynolds number range of a calibration in water a typical value of $Re_{\text{tap,throat}}$ is 3000 at which f is approximately equal to 3.8; so $f(Re_{\text{tap}})$ is written as $f^*(Re_{\text{tap}})$ +3.8 where $f^*(3000)$ is equal to 0. In water $Re_{\text{tap,up}}$ will be less than 3000, but the coefficient of f will be larger than 0.012. Assuming that

$$f^*(Re_{\text{tap}})=a(e^{-nRe_{\text{tap}}}-e^{-3000n}) \text{ for } Re_{\text{tap}}>3000 \quad (7)$$

the measured values of $C-C_{\text{water}}$ can be fitted, and the best fit of f^* to the gas data is

$$f^*(Re_{\text{tap}}) \quad (8)$$
$$=\begin{cases}7.165-8.839e^{-0.00007Re_{\text{tap}}} \text{ for } Re_{\text{tap}}>3000\\ 0 \text{ for } Re_{\text{tap}}\leq 3000.\end{cases}$$

This fit has an uncertainty based on two standard deviations of 0.0074. The true static hole error (rather than the difference between the static hole error in high-pressure gas and that in water) is based on

$$f(Re_{\text{tap}})=10.965-8.839e^{-0.00007Re_{\text{tap}}} \text{ for } Re_{\text{tap}}>3000 \quad (9)$$

and is shown in Fig. 10. Moreover, when the uncertainty of the complete equation (from Eqs. (1) and (6))

$$C=0.9878+0.0123\beta \quad (10)$$
$$+\frac{0.015f^*(Re_{\text{tap,throat}})-0.012\beta^4 f^*(Re_{\text{tap,up}})}{8(1-\beta^4)}$$

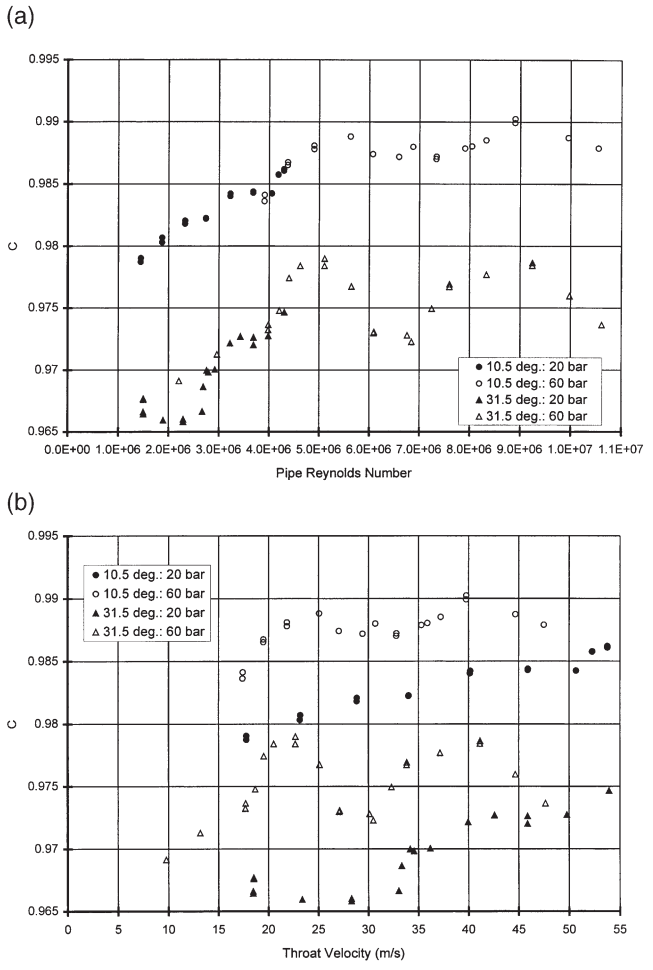

Fig. 9. (a) Calibration in gas against Reynolds number: β=0.75, 100 mm, non-standard convergent angles; (b) Calibration in gas against throat velocity: β=0.75, 100 mm, non-standard convergent angles.

with $f^*(Re_{tap})$ given by Eq. (8) is considered, the uncertainty (based on two standard deviations) of the complete database of values of C in gas is 1.24 per cent.

Similarly for a convergent angle of 10.5° the best fit of f^* to the gas data gives

$$f^*(Re_{tap}) = \begin{cases} 5.229 - 5.896e^{-0.00004Re_{tap}} & \text{for } Re_{tap} > 3000 \\ 0 & \text{for } Re_{tap} \le 3000. \end{cases} \quad (11)$$

This fit has an uncertainty based on two standard deviations of 0.0056. The true static hole error (rather than the difference between the static hole error in high-pressure gas and that in water) is based on

$$f(Re_{tap}) = 9.029 - 5.896e^{-0.00004Re_{tap}} \text{ for } Re_{tap} > 3000 \quad (12)$$

and is shown in Fig. 10. When the uncertainty of the complete equation

$$C = 0.9677 + 0.219\beta + \frac{0.015f^*(Re_{tap,throat}) - 0.012\beta^4 f^*(Re_{tap,up})}{8(1-\beta^4)} \quad (13)$$

with $f^*(Re_{tap})$ given by Eq. (11) is considered, the uncertainty (based on two standard deviations) of the complete database of values of C in gas is 0.76 per cent. This equation is based on the best fit to the mean discharge coefficients in water for a convergent angle of 10.5° (three points shown in Fig. 2) together with Eq. (6). This uncertainty is much lower than that obtained with the standard convergent angle, but is based on data from only three Venturi tubes.

For a convergent angle of 31.5° the best fit of f^* to the gas data gives

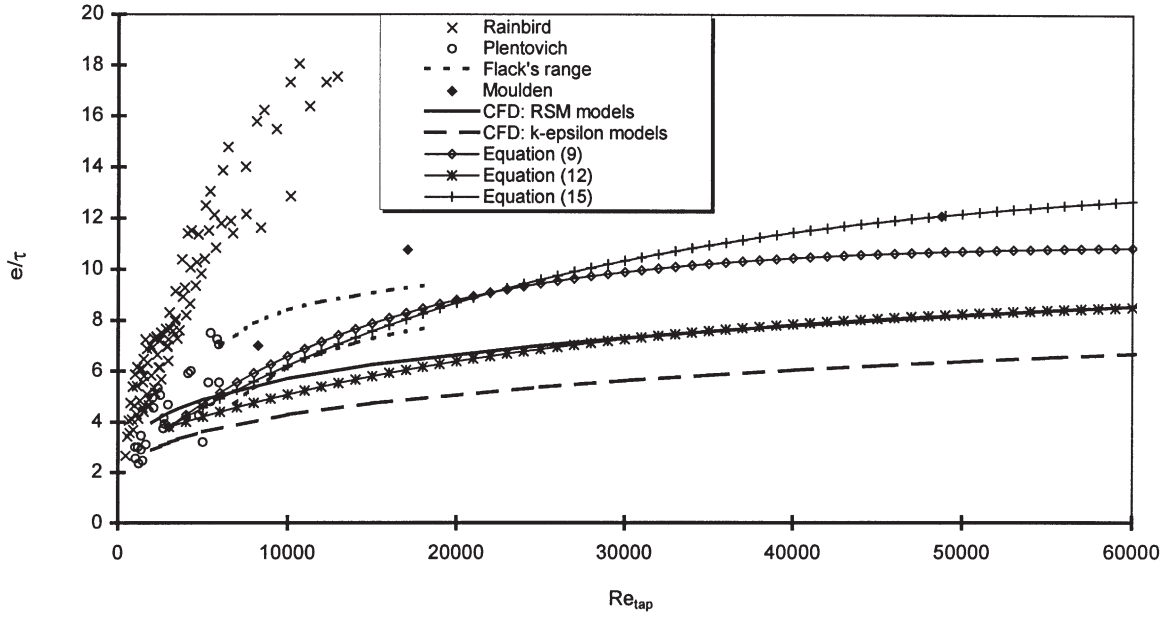

Fig. 10. Static hole error.

$$f^*(Re_{tap}) = \begin{cases} 9.879 - 11.138e^{0.00004Re_{tap}} & \text{for } Re_{tap} > 3000 \\ 0 & \text{for } Re_{tap} \le 3000. \end{cases} \quad (14)$$

This fit has an uncertainty based on two standard deviations of 0.0130. The true static hole error (rather than the difference between the static hole error in high-pressure gas and that in water) is based on

$$f(Re_{tap}) = 13.679 - 11.138e^{-0.00004Re_{tap}} \text{ for } Re_{tap} > 3000 \quad (15)$$

and is shown in Fig. 10. When the uncertainty of the complete equation

$$C = 1.0189 - 0.0619\beta + \frac{0.015f^*(Re_{tap,throat}) - 0.012\beta^4 f^*(Re_{tap,up})}{8(1-\beta^4)} \quad (16)$$

with $f^*(Re_{tap})$ given by Eq. (14) is considered, the uncertainty (based on two standard deviations) of the complete database of values of C in gas is 1.47 per cent. This equation is based on the best fit to the mean discharge coefficients in water for a convergent angle of 31.5° (three points shown in Fig. 2) together with Eq. (6).

None of the equations from Venturi tubes of different convergent angles is inconsistent with the data in Fig. 10 (see [7] for the CFD and [10–13] for the other data; the CFD results from many analyses have been represented by curve fits, as the sets of results were in good agreement with one another). This is encouraging in that there is a physical explanation for the discharge coefficient values measured in gas. Results at high Reynolds numbers, however, depend on other parameters besides Re_{tap}. This can be seen not only in the work done for this paper but also in the other experimental results, which are very varied at high Reynolds numbers, whereas (see [7]) good agreement between experimental data has been achieved at the Reynolds numbers obtained in water. Moreover, the cause of the peaks and troughs in the data is not clear: they may be the result of unsteady effects (e.g. acoustic effects), whereas the basic static hole error is a steady effect. These unsteady effects may lead not only to peaks and troughs, but also to a change in the static hole error from its basic value. The agreement between the CFD with the RSM turbulence model and Eq. (12), which is based on data with small peaks and troughs, suggests that for Venturi tubes with a convergent angle of 10.5° the basic static hole error model may be a very good model of the data in gas.

6. Practical equations

An alternative method of presenting the data which is easier to use than the method in Section 5 is to observe that the upstream static hole error term is much smaller than the throat term and that therefore it is possible simply to correlate the data with the throat tapping Reynolds number; the simplest presentation of this is to define the Venturi throat tapping Reynolds number

$$Re^* = \frac{d_{tap}}{d} Re_d. \quad (17)$$

The data for $C - C_{water}$ can then be plotted against Re^*, and Figs. 11–13 give the gas data for the standard convergent angle and for convergent angles of 10.5° and 31.5° respectively. Fitting the gas data for the standard convergent angle for $C - C_{water}$ gives:

$$C - C_{water} = \begin{cases} 0.0133 - 0.0169e^{-0.4(Re^*/10^5)} & Re^* > 60000 \\ 0 & Re^* \le 60000 \end{cases} \quad (18)$$

This is shown in Fig. 11. It has an uncertainty (based on two standard deviations) of 0.0074. When the corresponding overall equation

$$C = \begin{cases} 1.0011 + 0.0123\beta - 0.0169e^{-0.4(Re^*/10^5)} & Re^* > 60000 \\ 0.9878 + 0.0123\beta & Re^* \le 60000 \end{cases} \quad (19)$$

is compared with the database for C obtained in gas, it has an uncertainty (based on two standard deviations) of 1.23 per cent.

For a convergent angle of 10.5° fitting the gas data for $C - C_{water}$ gives

$$C - C_{water} = \begin{cases} 0.0085 - 0.0148e^{-0.4(Re^*/10^5)} & Re^* > 140000 \\ 0 & Re^* \le 140000 \end{cases} \quad (20)$$

This is shown in Fig. 12. It has an uncertainty (based on two standard deviations) of 0.0047. When the corresponding overall equation

$$C = \begin{cases} 0.9762 + 0.0219\beta - 0.0148e^{-0.4(Re^*/10^5)} & Re^* > 140000 \\ 0.9677 + 0.0219\beta & Re^* \le 140000 \end{cases} \quad (21)$$

is compared with the data for C obtained in gas, it has an uncertainty (based on two standard deviations) of 0.71 per cent. This figure is much lower than that obtained for Venturi tubes of standard convergent angle. It is necessary to establish that Eq. (21) is applicable for general use by undertaking further test work, since it is based on only three Venturi tubes. The standard deviation of the fit to the mean data for a convergent angle of 10.5° in water is 0.42 per cent.

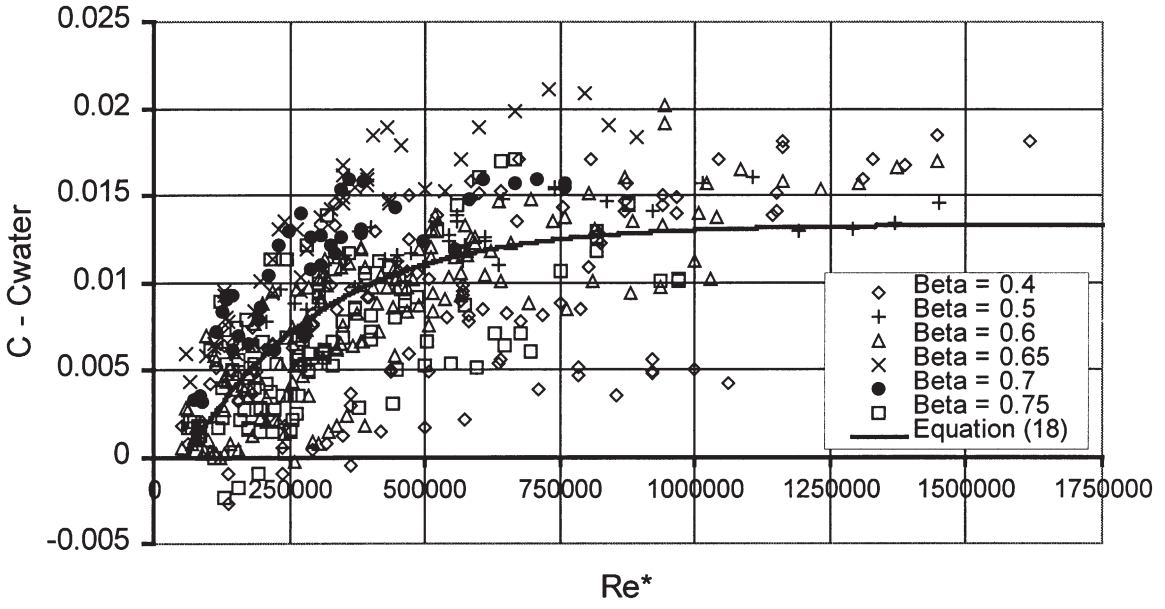

Fig. 11. $C-C_{water}$ with standard convergent angle.

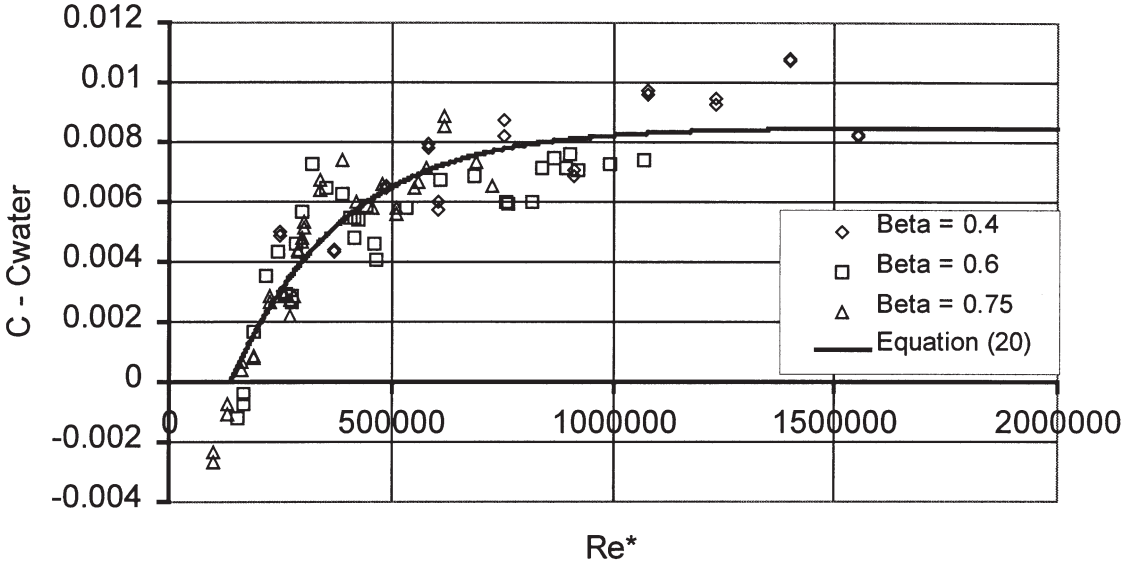

Fig. 12. $C-C_{water}$ with 10.5° convergent angle.

For a convergent angle of 31.5° fitting the gas data for $C-C_{water}$ gives

$$C-C_{water} = \begin{cases} 0.0161-0.0281e^{-0.4(Re^*/10^5)} & Re^*>140000 \\ 0 & Re^*\le 140000 \end{cases} \quad (22)$$

This is shown in Fig. 13. It has an uncertainty (based on two standard deviations) of 0.0102. This is more than twice the value for the Venturi tubes with 10.5° convergent angle.

When the corresponding overall equation

$$C= \begin{cases} 1.0350-0.0619\beta-0.0281e^{-0.4(Re^*/10^5)} & Re^*>140000 \\ 1.0189-0.0619\beta & Re^*\le 140000 \end{cases} \quad (23)$$

is compared with the data for C obtained in gas, it has an uncertainty (based on two standard deviations) of 1.36 per cent. The standard deviation of the fit to the mean data for a convergent angle of 31.5° in water is 0.79 per cent.

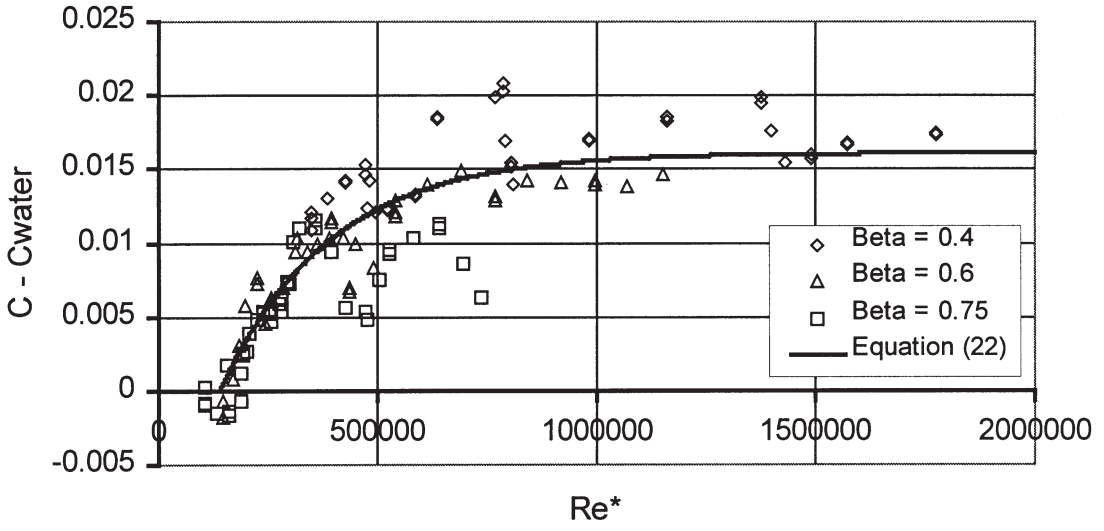

Fig. 13. $C-C_{water}$ with 31.5° convergent angle.

7. Conclusions

Twenty one Venturi tubes of a wide variety of diameters and diameter ratios have been made and calibrated in water and high-pressure gas. Fifteen of these are of the standard design, and an equation for the discharge coefficient in water has been obtained with an uncertainty of 0.74 per cent. This uncertainty is derived from the mean values of discharge coefficient for each Venturi tube and is based on 2 standard deviations of these mean values about the equation. In gas the situation is considerably more complicated. The recommended equation is Eq. (19) with Re^* defined in Eq. (17). This has an uncertainty of 1.23 per cent. The physical basis of this equation is static hole error theory. This provides a partial explanation of the measured discharge coefficients. Given the problems with the use of Venturi tubes in gas found in earlier work, this uncertainty is considered to be good.

The effect of changing the convergent angle of the Venturi tubes has been investigated and most encouraging results obtained with a convergent angle of 10.5°; indeed the gas data from the three Venturi tubes can be fitted with an uncertainty of 0.71 per cent by Eq. (21), which both has a physical basis and gives optimum results in water. This equation for Venturi tubes with a convergent angle of 10.5° is only based on three Venturi tubes; so further work in this area is desirable.

Further work on the effect of Venturi shape and of tapping diameter is being undertaken.

Acknowledgements

The work described in this paper was carried out as part of the Flow Programme, under the sponsorship of the National Measurement System Policy Unit of the United Kingdom Department of Trade and Industry. Their support is gratefully acknowledged.

This paper is published by permission of the Director, NEL.

References

[1] A.W. Jamieson, P.A. Johnson, E.P. Spearman, J. Sattary, Unpredicted behaviour of Venturi flowmeter in gas at high Reynolds numbers. In Proc. 14th North Sea Flow Measurement Workshop, Peebles, Scotland, 1996, paper 5.

[2] T. Van Weers, M.P. van der Beek, I.J. Landheer, C_d-factor of classical Venturi's: gaming technology? In Proc. 9th Int. Conf. on Flow Measurement, FLOMEKO, Lund, Sweden, 1998, pp. 203–207.

[3] M.J. Reader-Harris, W.C. Brunton, J.J. Gibson, D. Hodges, I.G. Nicholson, Venturi tube discharge coefficients. In Proc. 4th Int. Symposium on Fluid Flow Measurement, Denver, Colorado, 1999.

[4] M.J. Reader-Harris, W.C. Brunton, J.J. Gibson, D. Hodges, Discharge coefficients of Venturi tubes with non-standard convergent angles. In Proc. FLOMEKO 2000, Salvador, Brazil, 2000.

[5] International Organization for Standardization. Measurement of fluid flow by means of orifice plates, nozzles and Venturi tubes inserted in circular cross-section conduits running full. ISO 5167-1, Geneva: International Organization for Standardization, 1991.

[6] R.E. Franklin, J.M. Wallace, Absolute measurements of static-hole error using flush mounted transducers, J. Fluid Mech. 42 (1) (1970) 33–48.

[7] J.J. Gibson, M.J. Reader-Harris, A. Gilchrist, CFD analysis of the static hole error caused by tappings in Venturimeters operating in high-pressure gas. In Proc. 3rd ASME/JSME Joint Fluids Engineering Conference, San Francisco, FEDSM99-7149, 1999. New York: American Society of Mechanical Engineers.

[8] H. Schlichting, Boundary Layer Theory, McGraw-Hill, New York, 1960.

[9] D. Lindley, Venturimeters and boundary layer effects. PhD Thesis, Cardiff: Dept. of Mech. Eng., Univ. Coll. of South Wales and Monmouthshire, 1966.

[10] R.D. Flack, Jr. An experimental investigation of static pressure hole errors in transonic flow with pressure gradients. In Proc. Southeast Sem. on Thermal Science, 1978, pp. 364–378.

[11] T.H. Moulden, F.G. Wu, H.J. Collins, H. Ramm, C.I. Wu, R. Ray, Experimental study of static pressure orifice interference. AEDC TR-77-57, 1977.

[12] E.B. Plentovich, B.B. Gloss, Orifice-induced pressure error studies in Langley 7 by 10 foot high-speed tunnel. NASA Tech. Paper 2545, 1986.

[13] W.J. Rainbird, Errors in measurement of mean static pressure of a moving fluid due to pressure holes. Quart. Bull. Div. Mech. Eng., Nat. Res. Council, Canada, Rep. DME/NAE. No. 3, 1967.